



## Pharmacophore and docking-based combined *in-silico* study of KDR inhibitors

F.A. Pasha<sup>c,1</sup>, M. Muddassar<sup>c,d</sup>, M.M. Neaz<sup>c,d</sup>, Seung Joo Cho<sup>a,b,\*</sup>

<sup>a</sup> Research Center for Resistant Cells, Chosun University, Gwangju 501-759, Republic of Korea

<sup>b</sup> College of Medicine, Chosun University, 375 Seosuk-dong, Dong-gu, Gwangju 501-759, Republic of Korea

<sup>c</sup> Computational Science Center, Future Fusion Technology Division, Korea Institute of Science and Technology, PO Box 131, Seoul 130-650, Republic of Korea

<sup>d</sup> University of Science and Technology, 113 Gwahangno, Yuseong-gu, Daejeon, Korea

### ARTICLE INFO

#### Article history:

Received 25 September 2008

Received in revised form 22 March 2009

Accepted 11 April 2009

Available online 19 April 2009

#### Keywords:

3D-QSAR

Drug design

Pharmacophore

Docking

CoMFA

CoMSIA

VEGFR

### ABSTRACT

The growth and metastasis of solid tumors is dependent on angiogenesis. The vascular endothelial growth factor (VEGF) and its cell surface receptor in human KDR (kinase domain containing receptor or VEGFR-2) have particular interest because of their importance in angiogenesis. The development of novel inhibitors of VEGFR-2 would be helpful to check the growth of tumors. Quantitative structure activity relationship (QSAR) analyses used to understand the structural factors affecting inhibitory potency of thiazole-substituted pyrazolone derivatives. Several pharmacophore-based models indicated the importance of steric, hydrophobic and hydrogen bond acceptor groups to inhibitory activity. The comparative molecular field analyses (CoMFA) and comparative molecular similarity indices analyses (CoMSIA) based 3D-QSAR models were derived using pharmacophore-based alignment. Both CoMFA ( $q^2 = 0.70$ ,  $r^2 = 0.97$  and  $r^2_{\text{predictive}} = 0.61$ ) and CoMSIA ( $q^2 = 0.54$ ,  $r^2 = 0.82$  and  $r^2_{\text{predictive}} = 0.66$ ) gave reasonable results. The molecular docking (receptor-guided technique) with a recently reported receptor structure (PDB = 1YWN) were performed. The docked alignment was subsequently used for 3D-QSAR (CoMFA;  $q^2 = 0.56$ ,  $r^2 = 0.97$ ,  $r^2_{\text{predictive}} = 0.82$ , CoMSIA;  $q^2 = 0.58$ ,  $r^2 = 0.91$ ,  $r^2_{\text{predictive}} = 0.69$ ). The overall both studies were indicated, steric, electrostatic and hydrogen bond acceptor effects contribute to the inhibitory activity. CoMFA and CoMSIA models suggested that a positive bulk with hydrophobic effect is desirable around position 4 and 5 and hydrogen bond acceptor groups around pyrazolones ring will be helpful.

© 2009 Elsevier Inc. All rights reserved.

### 1. Introduction

Angiogenesis is a physiological process involving the growth of new blood vessels from pre-existing vessels. It occurs during tissue growth from embryonic development to maturity, after which the process enters a period of relative quiescence during adulthood. Angiogenesis is also activated during wound healing and at certain stages of the female reproductive cycle [1]. One of the most extensively studied pathways in this area is vascular endothelial growth factor (VEGF) [2] and its cell surface receptor in human KDR (kinase domain containing receptor or VEGFR-2) [3,4] due to their important roles in angiogenesis [5]. This is vital for survival and proliferation of tumor cells. KDR receptors, shown to be expressed

primarily in endothelial cells [6] upon binding to VEGF, get activated and their intracellular kinase domains undergo auto-phosphorylation, which in turn triggers signaling pathways leading to sprouting of blood vessels toward the tumor cells. Therefore, inhibition of KDR kinase and subsequent blockage of angiogenesis could be an alternate approach to cancer therapy. Several small molecular VEGFR-2 inhibitors [7,8] have emerged as promising anti-angiogenic agents for possible treatment against a wide variety of cancers [9]. One of the pioneering class of compounds belongs to 1,2,3-thiadiazole substituted pyrazolones. To explore further possibilities we used different quantitative structure activity relationship (QSAR) techniques, which are also in our practice [10–15]. The current study deals ligand-based and receptor-guided QSAR techniques. The ligand-based study was performed using pharmacophore techniques with PHASE module [16] and the receptor-guided study was performed using molecular docking techniques with GLIDE. A recently reported co-crystal structure (1YWN) [17] obtained from protein data bank and used as receptor structure. Additionally the 3D-QSAR (comparative molecular field analysis (CoMFA) and comparative

\* Corresponding author.

E-mail addresses: [fpasha@rediffmail.com](mailto:fpasha@rediffmail.com) (F.A. Pasha), [chosj@chosun.ac.kr](mailto:chosj@chosun.ac.kr) (S.J. Cho).

<sup>1</sup> Current Address: Institute de Biologie Structurale, 41, rue Jules horowitz, Grenoble-Cedex-38027, France.

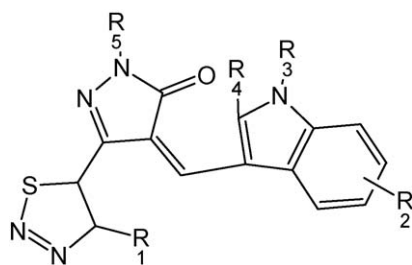


Fig. 1. The basic skeleton of pyrazolone compounds.

molecular similarity indices analysis (CoMSIA) [18,19] have been performed to understand the possible interaction involved in ligand binding with KDR.

## 2. Material and methods

### 2.1. Data sets

Fig. 1 displayed parent structure of thiazole-substituted pyrazolones. Thirty-three such novel inhibitors of VEGFR-2 were taken from literature [20] with their biological activities in terms of  $IC_{50}$  values ( $IC_{50}$  values, i.e., the concentration ( $\mu M$ ) of inhibitor that produces 50% inhibition of VEGFR-2) accordingly the  $pIC_{50}$  ( $-\log IC_{50}$ ) reported in Table 1. The data set divided into a training set of 23 molecules and test set of 10 molecules. Ligand-based and receptor-guided 3D-QSAR models were developed using pharmacophore identification and molecular docking method, respectively.

### 2.2. Generation of the common pharmacophore hypothesis (CPH)

The common pharmacophore hypotheses (CPH) were generated using PHASE [16]. Conformers were generated using MCM/

**Table 1**  
The molecular structure and observed activities [21] of pyrazolones.

No.	R <sub>1</sub>	R <sub>2</sub>	R <sub>3</sub>	R <sub>4</sub>	R <sub>5</sub>	$IC_{50}$ (nM)	$pIC_{50}$
1	CH <sub>3</sub>	H	H	H	H	1000	-3.00
2	CH <sub>3</sub>	H	CH <sub>3</sub>	H	H	95	-1.98
3	CH <sub>3</sub>	5-F	CH <sub>3</sub>	H	H	99	-2.00
4	CH <sub>3</sub>	5-Cl	CH <sub>3</sub>	H	H	152	-2.18
5	CH <sub>3</sub>	5-Cl	H	H	H	300	-2.48
6	CH <sub>3</sub>	5-OCH <sub>3</sub>	CH <sub>3</sub>	H	H	90	-1.95
7	CH <sub>3</sub>	5-CN	CH <sub>3</sub>	H	H	300	-2.48
8	CH <sub>3</sub>	4-F	CH <sub>3</sub>	H	H	137	-2.14
9	CH <sub>3</sub>	4-Cl	CH <sub>3</sub>	H	H	45	-1.65
10	CH <sub>3</sub>	4-Br	CH <sub>3</sub>	H	H	34	-1.53
11	CH <sub>3</sub>	4-OCH <sub>3</sub>	CH <sub>3</sub>	H	H	19	-1.28
12	CH <sub>3</sub>	4-OC <sub>2</sub> H <sub>5</sub>	CH <sub>3</sub>	H	H	38	-1.58
13	CH <sub>3</sub>	4-CH <sub>3</sub>	CH <sub>3</sub>	H	H	58	-1.76
14	CH <sub>3</sub>	4-Br,5-OCH <sub>3</sub>	CH <sub>3</sub>	H	H	23	-1.36
15	CH <sub>3</sub>	7-OCH <sub>3</sub>	CH <sub>3</sub>	H	H	109	-2.04
16	CH <sub>3</sub>	4,7-bis-OCH <sub>3</sub>	CH <sub>3</sub>	H	H	20	-1.30
17	H	5-F	CH <sub>3</sub>	H	H	48	-1.68
18	H	5-Cl	CH <sub>3</sub>	H	H	34	-1.53
19	H	5-CN	CH <sub>3</sub>	H	H	174	-2.24
20	H	5-COOCH <sub>3</sub>	CH <sub>3</sub>	H	H	73	-1.86
21	H	5-OCH <sub>3</sub>	CH <sub>3</sub>	H	H	28	-1.45
22	H	5-Br	CH <sub>3</sub>	H	H	110	-2.04
23	H	5-CH <sub>3</sub>	CH <sub>3</sub>	H	H	35	-1.54
24	H	4-F	CH <sub>3</sub>	H	H	16	-1.20
25	H	4-Cl	CH <sub>3</sub>	H	H	16	-1.20
26	H	4-Br	CH <sub>3</sub>	H	H	8	-0.90
27	H	4-OCH <sub>3</sub>	CH <sub>3</sub>	H	H	13	-1.11
28	H	4-OC <sub>2</sub> H <sub>5</sub>	CH <sub>3</sub>	H	H	25	-1.40
29	H	4-COOCH <sub>3</sub>	CH <sub>3</sub>	H	H	22	-1.34
30	H	4-Br, 5-OCH <sub>3</sub>	CH <sub>3</sub>	H	H	6	-0.78
31	H	6-Cl	CH <sub>3</sub>	H	H	73	-1.86
32	H	4-Br, 6-CH <sub>3</sub>	CH <sub>3</sub>	H	H	12	-1.08
33	H	4,7-bis-OCH <sub>3</sub>	CH <sub>3</sub>	H	H	10	-1.00

LMOD with OPLS-2005 force field [21]. The most dominating features, hydrogen bond acceptor (A), hydrogen bond donor (D), hydrophobic group (H), negatively charged group (N), positively charged group (P), and aromatic ring (R), were defined by a set of chemical structural patterns. Pharmacophore matching tolerance was 1 Å. Those CPHs considered, which indicated at least five sites common to all 33 molecules. Further, the best CPH was selected because of survival score.

### 2.3. Assessment of significant CPHs using partial least square (PLS) analyses

The evaluation of generated CPHs performed by correlating the observed and estimated activity for the training set of 23 molecules and test set of 10 molecules. Partial least square (PLS) analyses performed using strike with maximum N/3 PLS factors, N1/3 number of ligands in training set, and either atom, or pharmacophore-based model using grid spacing of 1 Å. CPHs of significant statistical values were selected for molecular alignments to use in ligand-based CoMFA and CoMSIA.

### 2.4. Molecular docking

The crystal structure of VEGFR-2 (PDB = 1YWN) was used as receptor for molecular docking studies. The inhibitor structure was minimized using OPLS-2005 [21] force field in Macro Model. The molecular docking performed using GLIDE docking tool with standard protocols. The active site was defined within 5Å surrounding to the co-crystallized ligand and the specific residues and constraints information were obtained from crystallographic data as well as an earlier study [20]. The final ligand binding poses were ranked according to a computed model score that encompasses the grid score, proprietary GLIDE score, and the internal energy strain. The inhibitors were docked in to the receptor site using GLIDE docking algorithm in the SP (standard precision) mode. Docked geometry based alignment was used for receptor-guided CoMFA and CoMSIA.

### 2.5. 3D-QSAR

The 3D-QSAR models were developed using CoMFA and CoMSIA techniques.

### 2.6. CoMFA and CoMSIA

The initial setup for CoMFA and CoMSIA was similar to our earlier work [10,22,23]. In summary CoMFA were studied using steric and electrostatic potential fields while CoMSIA was based on five different properties (steric, electrostatic, hydrophobic, H-bond donors and acceptors). All the calculations were performed using Sybyl software [24].

### 2.7. Partial least square (PLS) analysis and validation of QSAR models

To derive 3D-QSAR models, the CoMFA and CoMSIA descriptors were used as independent variables and the  $pIC_{50}$  values as dependent variable. PLS method [25,26] was used to linearly correlate these CoMFA and CoMSIA descriptors to the activity. The basic statistical setup was same as defined in our earlier works [10,22,27]. To have robustness and statistical confidence of the derived models, bootstrapping analysis used for 10 runs. To assess the predictive power of the derived 3D-QSAR models, activity of test set of 10 molecules were predicted. The predictive abilities of the models expressed by the predictive  $r^2$  value, which is analogous to cross-validated  $r^2(q^2)$ .

Download English Version:

<https://daneshyari.com/en/article/444588>

Download Persian Version:

<https://daneshyari.com/article/444588>

[Daneshyari.com](https://daneshyari.com)